

# Entanglement transition of elastic lines in a strongly disordered environment

Viljo Petaja,<sup>1</sup> Mikko Alava,<sup>1,2</sup> and Heiko Rieger<sup>3</sup>

<sup>1</sup> Helsinki University of Techn., Lab. of Physics, P.O. Box 1100, 02015 HUT, Finland

<sup>2</sup> SM C-INFM, Dipartimento di Fisica, Università "La Sapienza", P.le A. Moro 2 00185 Roma, Italy

<sup>3</sup> Theoretische Physik, Universität des Saarlandes, 66041 Saarbrücken, Germany

We investigate by exact optimization the geometrical properties of three-dimensional elastic line systems with point disorder and hard-core repulsion. The line 'forests' become entangled due to increasing line wandering as the system height is increased, at fixed line density. There is a transition height at which a cluster of pairwise entangled lines spans the system, transverse to average line orientation. Numerical evidence implies that the phenomenon is in the ordinary percolation universality class.

PACS numbers: 74.60.Ge, 05.40.-a, 74.62.Dh

The topological entanglement of line-like elastic objects is an important physical phenomenon for a number of interacting many-body systems. Examples are the entanglement of magnetic flux lines in high- $T_c$  superconductors in the mixed phase [1, 2] or the entanglement of polymers in materials like rubber [3]. The degree of entanglement of the lines usually manifests itself in various measurable properties like stiffness or shear modulus in the case of polymers and in transport or dynamical properties for magnetic flux lines in superconductors.

In the latter case the entanglement is caused either by thermal fluctuations [1, 4] or sufficiently strong quenched disorder through lattice defects or pinning centers [5, 6]. It varies with the line density which is proportional to the square-root of the strength of the applied magnetic field. A strongly disordered high- $T_c$  superconductor is in a vortex glass state [7], which is superconducting (or has at least an extremely small resistivity) and in which the Abrikosov flux line lattice is destroyed as in the non-superconducting vortex liquid state. At weaker disorder or at smaller magnetic fields a transition to a Bagg glass phase [8], in which the positions of the flux lines show quasi-long-range order, takes place. This has been observed experimentally [9] and in simulations [10]. In contrast to this (quasi)-ordered solid, the lines in the vortex glass phase are expected to be strongly entangled [11, 12]. An elastic description, the starting point for the theory of the Bagg glass phase [8], is inappropriate due to the proliferation of topological defects. A theoretical understanding of this topologically highly non-trivial state including the conditions under which it occurs is highly desirable.

In this paper we study a model for such an ensemble of elastic lines exposed to strong point disorder and focus on the transition from independent lines to entangled bundles of lines. Due to the disorder potential the lines make transverse excursions even in the absence of thermal fluctuations and wind around each other. We introduce a computationally convenient measure for the entanglement of two lines via their winding angle and study clusters of mutually entangled lines, since the physical

properties of the line system are expected to change drastically (if compared with an unentangled, Bagg-glass like case) when the size of these clusters grow. Beyond a particular height of the system, which depends on the line density, a percolating bundle of entangled lines is formed. It spans the whole transverse system size representing a disorder induced braided flux phase. Thus, in accordance with an observation by Nelson for the thermal case [1], in sufficiently thin samples the line system will behave like disentangled rods (still pinned by the disorder), whereas for sufficiently thick systems the lines will undergo an entanglement transition. This takes place also if the line density is varied, e.g. in high- $T_c$  superconductors, by increasing the magnetic field. This transition may be the one observed experimentally [9] from a Bagg glass phase to an entangled vortex glass phase.

We consider the following model for a three-

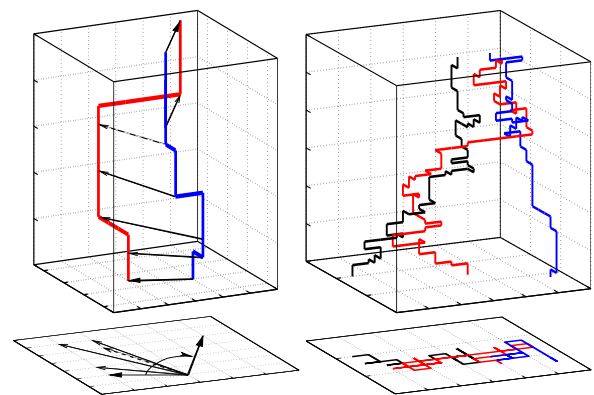


FIG. 1: Left: Definition of the winding angle of two flux lines: For each  $z$ -coordinate the vector connecting the two lines is projected onto that basal plane.  $z = 0$  gives the reference line with respect to which the consecutive vectors for increasing  $z$ -coordinate have an angle  $\alpha(z)$ . Once  $\alpha(z) > 2\pi$  the two lines are said to be entangled. Right: Top: A configuration of three lines that are entangled (n.b.: scale of  $z$ -axis is strongly reduced). Bottom: The projection of the line configuration on the basal plane, defining a connected cluster.

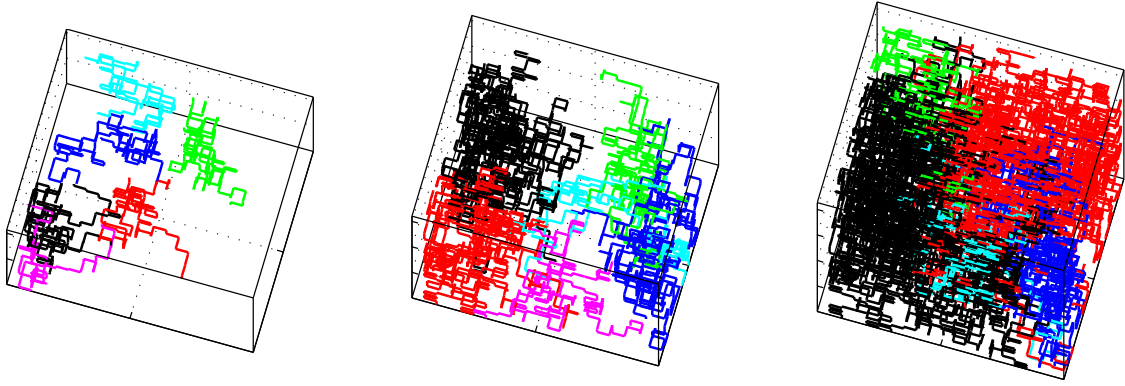


FIG. 2: Line configurations for different heights  $H$  (from left to right:  $H = 64, 96, 128$ ), the lateral size  $L = 20$ , the line density is  $\rho = 0.3$ . Only the largest line bundles are shown, indicated by a varying grey scale. Black denotes the largest cluster, which eventually percolates.

dimensional system of interacting lines in a disordered environment: The lines live on the bonds of a simple cubic lattice with a lateral width  $L$  and a longitudinal height  $H$  ( $L \times L \times H$  sites) with free boundary conditions in all directions. Each line starts and ends at an arbitrary position on the bottom respective top planes. The number  $N$  of lines threading the sample is fixed by a prescribed density  $\rho = N/L^2$ . The lines have hard-core interactions, so that their configuration is specified by bond-variables  $n_i \in \{0, 1\}$ ;  $n_i = 1$  indicates that a line segment occupies bond with index  $i$ , while  $n_i = 0$  means the bond is vacant. Note that we allow line crossing at the lattice sites, and thus the line identification based upon a bond configuration is not unique.

We model the disordered environment by assigning a random (potential) energy  $e_i \in [0, 1]$  (uniformly distributed) to each bond  $i$ . The total energy of the line configuration is given by

$$H = \sum_i e_i n_i \quad (1)$$

An elastic energy term is intrinsically present in this model (i.e. is generated upon coarse graining) since the positivity of the energies  $e_i$  disfavor in general large transverse excursions of the lines. An equivalent continuum version of this model is

$$H = \sum_{i=1}^N \int_0^H dz \left[ \frac{\rho}{2} \left( \frac{dr_i}{dz} \right)^2 + \sum_{j \neq i} V_{\text{int}}[r_i(z) - r_j(z)] + V_r[r_i(z); z] \right] \quad (2)$$

where  $r_i(z)$  denotes the transversal coordinate at longitudinal height  $z$  of the  $i$ -th flux line and where, in order to reduce to the lattice version the interactions  $V_{\text{int}}[r_i(z) - r_j(z)]$  have to be short ranged (i.e. in case of flux lines the screening length small compared to the average line distance) or just hard core repulsive, and the

random,  $\delta$ -correlated disorder potential  $V_r[r_i(z); z]$  has to be strong compared to the elastic energy ( $\rho$ ).

At low temperatures the line configurations will be dominated by the disorder and thermal fluctuations are negligible. We focus ourselves to zero temperature, the ground state of the energy (1). The computation thereof is a non-trivial task and can not be handled in an iterative manner by solving successive single line problems. We use an exact polynomial combinatorial optimization algorithm [13, 14].

The resulting line configuration is then analyzed. We compute the winding angle of all line pairs as indicated in Fig. 1 (c.f. [15]). We define two lines to be entangled when this winding angle becomes larger than  $2\pi$ . This choice is one that measures entanglement from the topological perspective ([12]), and comes from the requirement that an entangled pair of lines can not be separated by a suitable linear transformation in the basal plane (i.e. the lines almost always would cut each other, if one were shifted). The precise definition of entanglement is not of major relevance, and the one used is useful since it is the computationally easiest.

Sets or bundles of pairwise entangled lines are formed so that a line belongs to a bundle if it is entangled at least with one other line in the set. The topological multi-line-entanglement could be characterized by other measures as well; the universal properties of the transition will not depend on these. These line bundles are spaghetti-like | i.e. topologically complicated and knotted sets of one-dimensional objects. To study the size distribution of these objects we project these bundles on the basal plane, as indicated in Fig. 1, where a bundle projects onto a connected cluster. The probability for two lines to be entangled increases with increasing system height. Consequently one would expect that the bundle size increases with  $H$ , and therefore also their projections, the clusters. This scenario is exemplified in Fig. 2, for the largest height the largest cluster spans from one side of

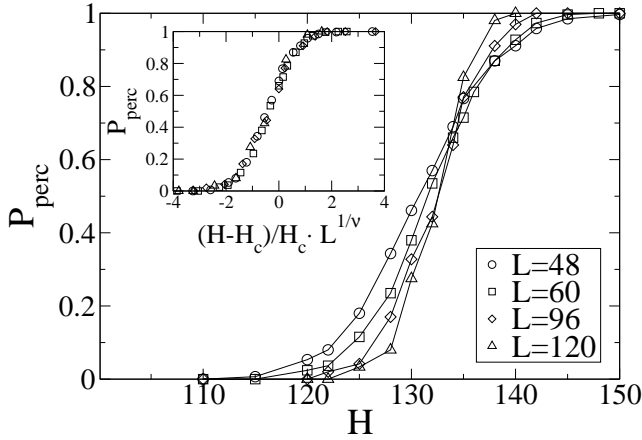


FIG. 3: Percolation probability for different lateral system sizes  $L$  as a function of the system height  $H$ , the line density is  $\rho = 0.3$ . Inset: Scaling plot of the data with  $H_c = 134$  and  $\nu = 4/3$ .

the system to the other, i.e. it percolates.

Hence, for a given line density we expect that for system heights larger than a critical value  $H_c$  a system spanning large entangled bundle occurs, containing an infinite number of lines in the limit  $L \rightarrow \infty$ . We will call this an entanglement transition occurring at a finite system height  $H_c$ . In the projection plane this appears like a percolation transition and in the following we will investigate its universal properties.

The numerical data we present have been obtained by averaging over up to  $10^3$  realizations of the random potentials  $e_i$  in (1) and the statistical error resulting from this finite sample average is in all cases smaller than the symbol size. We studied different line densities between  $\rho = 0.1$  and  $\rho = 0.5$ , but present for brevity only data for  $\rho = 0.3$ . The  $\rho$ -dependence of the non-universal quantities like  $H_c$  is discussed later | the exponents we report are universal, i.e.  $\rho$ -independent.

In Fig. 3 we show the probability  $P_{\text{perc}}$  of the clusters, formed by the entangled bundles in the projection plane, to percolate as a function of the height  $H$  of the system. The curves for different lateral system sizes  $L$  intersect at  $H_c$ , which gives our estimate for  $H_c(\rho = 0.3) = 134$ . The inset shows a scaling plot according to

$$P_{\text{perc}} = p(L^{-1/\nu}) \quad (3)$$

with  $x = (H - H_c)/H_c$  the reduced distance from the critical height and  $\nu = 4/3$  the correlation length exponent. The finite size corrections for smaller system sizes than those shown are large, but could be incorporated in the scaling plot by using an  $L$ -dependent shift  $H_c(L)$  that converges to  $H_c$  for large  $L$ .

$\nu = 4/3$  is the exponent of conventional bond perco-

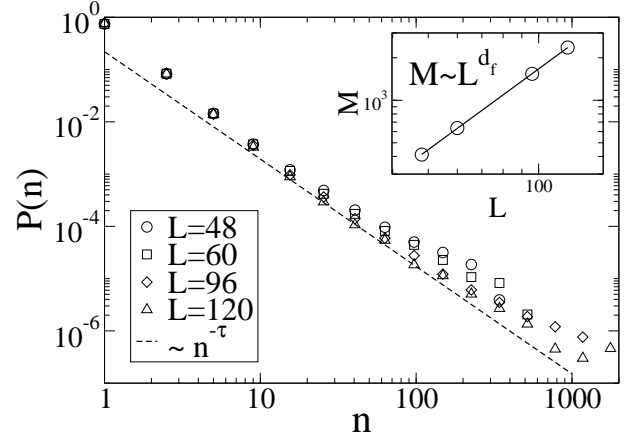


FIG. 4: Cluster size distributions for different lateral system size at the percolation height  $H_c = 134$  in log-log plot. One sees the finite size effects in the tails, the broken line has slope  $\tau = 2.06$  and fits the asymptotic  $(L \rightarrow \infty) P(n)/n$ . Inset: Log-log-plot of the mass (number of entangled lines) of the percolating cluster at  $H_c = 134$  as a function of the lateral size  $L$ . The straight line has slope  $d_f = 1.90$ , the fractal dimension of percolation.

lation in two dimensions. Thus we are led to the conclusion that the entanglement transition belongs to the same universality class as conventional 2d percolation. We checked other quantities to confirm this result: Fig. 4 shows the cluster size distribution  $P(n)$  at  $H = H_c$  for various lateral system sizes  $L$  and we find that it approaches

$$P(n)/n \quad \text{with} \quad \tau = 187/91 = 2.055 \quad (4)$$

in the limit  $L \rightarrow \infty$ . The inset shows the mass (i.e. number of entangled lines) of the percolating bundle at  $H_c$ , which fits well to

$$M \sim L^{d_f} \quad \text{with} \quad d_f = 91/48 = 1.896 \quad (5)$$

Both exponents, the cluster distribution exponent  $\tau$  and the fractal dimension  $d_f$  are identical to those for conventional bond percolation and one can also use the order parameter exponent,  $\beta = 5/36$ , to fit the data reasonably well.

This result is somewhat surprising, since naively one would expect that the processes that lead to the entanglement of two lines might create substantial correlations, and since these, if long ranged, would change the universality class of the percolation transition [16]. One indication that this is not the case is given by the probability for two lines with mass center distance  $r$  to be entangled,  $P_{>2}(r)$ , which we show in Fig. 5. It decays exponentially with  $r$ , implying at least for two-line-entanglement only short range correlations. It scales

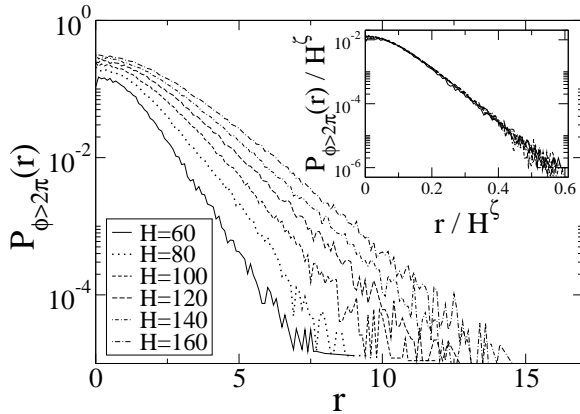


FIG. 5: Probability  $P_{>2\pi}(r)$  that two lines at a mass center distance  $r$  have a winding angle larger than  $2\pi$ , i.e. are entangled. Inset: Scaling plot, according to  $P_{>2\pi}(r) = H^{-\zeta} \tilde{P}(r/H^{\zeta})$ .  $\zeta = 0.62$  is the single line roughness exponent. The lateral system size is  $L = 96$ , since  $r \leq L$  there is no finite length effect.

with the typical size of the transverse fluctuations of a single line  $H^{\zeta}$ , where  $\zeta = 0.62$  is the roughness exponent for a single line in a random environment [17, 18], so that  $P_{>2\pi}(r) = H^{-\zeta} \tilde{P}(r/H^{\zeta})$ . It is noteworthy that the scaling implies the lines contributing considerably to entanglement follow a scaling stemming from single-line behavior. We studied also three-line correlations (e.g. the probability of a third line to be entangled with one or two others, given that these two are entangled or not), and found that they are also only short-ranged.

The critical height,  $H_c$ , above which an extensive portion of lines is entangled (an infinite cluster would occur in the infinite system) varies non-monotonically with the line density. We expect that  $H_c \rightarrow 1$  in both limits  $\rho \rightarrow 0$ , i.e. very dilute system, and  $\rho \rightarrow 1$ , very dense systems. In the former case simply because the typical individual line fluctuations  $w/H$  should be of the same order of magnitude as the typical line-to-line distance  $d = 1/\rho$ . For this the height has, obviously, to be large enough. In the opposite limit of a dense system the effective stiffness starts to increase due to the hard core interactions (i.e. a lack of vacancies, or unoccupied bonds). Hence  $H_c(\rho)$  has a minimum between these two limits and it turns out to be around  $\rho = 0.4$ . Our estimates for the critical exponents are independent of  $\rho$ , for the values considered, but the quality of the data deteriorates since greater system heights or a larger density means fewer samples. We expect that for all the entanglement transition is in the percolation universality class.

To conclude we studied the entanglement transition of hard core repulsive lines in a disordered environment as a function of the system height. This transition is

equivalently driven by the line density, and then we find two transitions or a non-monotonic behavior of  $H_c(\rho)$ , for sufficiently thick samples. The one at low densities we would argue to be related to the the Bragg to vortex glass transition in high- $T_c$  superconductors [9, 10]. A signature of this would be a dependence of the order-disorder phase boundary on the sample thickness. The transition is characterized by the formation of an extensive line bundle. It will play the role of a topological obstacle for also those lines that are not part of it, due to the energy cost of vortex-vortex cutting. It would be interesting to study the modifications of the entanglement transition due to splayed line defects [6], or other forms of correlated disorder. Moreover, it would be highly desirable to include long-range interactions among the lines, since only in their presence a Bragg glass phase on the low disorder or low line density side will occur. The addition of thermal fluctuations, which we neglected here, will lead to another interesting transition, from an entangled vortex glass to an entangled vortex liquid.

We acknowledge gratefully the support of the European Science foundation (ESF) SPHINX network, the Deutsche Forschungsgemeinschaft (DFG), and (MJA, VIP) the Center of Excellence program of the Academy of Finland.

- 
- [1] D. R. Nelson, Phys. Rev. Lett. 60, 1973 (1988).
  - [2] For a review see G. Blatter et al., Rev. Mod. Phys. 66, 1125 (1994).
  - [3] M. Doi and S. F. Edwards, The theory of Polymer Dynamics, (Oxford University Press, Oxford, 1986).
  - [4] Y.-H. Li and S. Teitel, Phys. Rev. B 49, 4136 (1994); A. K. Nguyen, A. Sudbo, and R. E. Hetzel, Phys. Rev. Lett. 77, 1592 (1996); H. Nordborg and G. Blatter, Phys. Rev. Lett. 79, 1925 (1997) and Phys. Rev. B 58, 14556 (1998); Y. Nonomura, X. Hu, and M. Tachiki, Phys. Rev. B 59, R11657 (1999).
  - [5] S. P. Obukhov and M. Rubinstein, Phys. Rev. Lett. 65, 1279 (1990).
  - [6] T. Hwa, P. Le Doussal, D. R. Nelson, and V. M. Vinokur, Phys. Rev. Lett. 71, 3545 (1993).
  - [7] M. P. A. Fisher, Phys. Rev. Lett. 62, 1415 (1989); D. S. Fisher et al, Phys. Rev. B 43, 130 (1991).
  - [8] T. Nattermann, Phys. Rev. Lett. 64, 2454 (1990); T. Giamachi and P. Le Doussal, Phys. Rev. Lett. 72, 1530 (1994); and Phys. Rev. B 52, 1242 (1995).
  - [9] B. K. Haykovich et al., Phys. Rev. Lett. 76, 2555 (1996); K. Deligiannis et al., Phys. Rev. Lett. 79, 2121 (1997); I. Joumard et al., Phys. Rev. Lett. 82, 4930 (1999); Y. Paltiel et al., Phys. Rev. Lett. 85, 3712 (2000).
  - [10] Y. Nonomura and X. Hu, Phys. Rev. Lett. 85, 5140 (2001).
  - [11] K. V. Samokhin, Phys. Rev. Lett. 84, 1304 (2000).
  - [12] R. Bikbov and S. Nechaev, Phys. Rev. Lett. 87, 150602 (2001).
  - [13] H. Rieger, Phys. Rev. Lett. 81, 4488 (1998).
  - [14] M. A. Lava, P. Duxbury, C. M.oukarzel and H. Rieger: Combinatorial optimization and disordered systems,

- \Phase Transitions and Critical Phenomena", vol. 18., (ed. C. Domb and J. L. Lebowitz) (Academic Press, 2000); A. Hartmann and H. Rieger, Optimization Algorithms in Physics, (Wiley VCH, Berlin, 2002).
- [15] B. Drossel and M. Kardar, Phys. Rev. E 53, 5861 (1996).
- [16] A. Weinrib, Phys. Rev. B 29, 387 (1984).
- [17] T. Halpin-Healy and Y.-C. Zhang, Physics Reports 254, 215 (1995).
- [18] J. M. Kin, M. A. Moore and A. J. Bray, Phys. Rev. A 44, 2345 (1991); N. Schwartz, A. L. Nazaryev and S. Havlin, Phys. Rev. E 58, 7642 (1998); E. Perlmutter and S. Havlin, Phys. Rev. E 63, 010102 (2001).